ISSN 0742-0463, Journal of Volcanology and Seismology, 2018, Vol. 12, No. 6, pp. 359–378. © Pleiades Publishing, Ltd., 2018.
Original Russian Text © A.V. Volkov, A.A. Sidorov, V.Yu. Prokofiev, N.E. Savva, E.E. Kolova, K.Yu. Murashov, 2018, published in Vulkanologiya i Seismologiya, 2018, No. 6, pp. 3–22.

Epithermal Mineralization in the Okhotsk–Chukchi Volcano-Plutonic Belt

A. V. Volkov[a, *], A. A. Sidorov[a], V. Yu. Prokofiev[a], N. E. Savva[b], E. E. Kolova[b], and K. Yu. Murashov[a]

[a] *Institute of Geology of Ore Deposits, Petrography, Mineralogy, and Geochemistry, Russian Academy of Sciences, Staromonetnyi per., 35, Moscow, 119017 Russia*
[b] *Northeast Multidisciplinary Institute, Far East Branch, Russian Academy of Sciences, ul. Portovaya, 16, Magadan, 685010 Russia*
**e-mail: tma2105@mail.ru*

Received February 8, 2018

Abstract—This paper considers the geochemistry and conditions of generation for the Mesozoic Au–Ag epithermal deposits in the Okhotsk–Chukchi volcanic–plutonic belt (OChVB) in Northeast Russia. We provide new data on the composition and concentrations of trace elements, including REEs, in the ores of epithermal Au–Ag deposits. The ores were found to be enriched in a wide range of trace elements. The REE distributions of these ores are dominated by light "hydrophile" lanthanoids of the "cerium" group. The Eu anomalies were found to vary between high negative to low and high positive levels. Comparative analysis over the classes of gold concentration showed a synchronous enrichment of the ores in similar sets of trace elements. A study of fluid inclusions revealed that the ore-forming solutions had hydrocarbonate potassium or hydrocarbonate sodium compositions. The fluids had high concentrations of sulfate ions for most deposits. The salinity of the fluids was frequently found to increase toward later low-temperature mineralization phases. We identified the tendency of increasing K^+ percentage in the fluid from the earlier oreless quartz to productive quartz with increasing depth, as well as some decrease in the percentages of Na^+, Ca^{++}, and Cl^-. The results indicate magma chambers of andesite magmas and meteoric waters as the most likely sources of the fluids that generated the epithermal Au–Ag ores in the OChVB deposits.

DOI: 10.1134/S0742046318060088

INTRODUCTION

The older placer areas are sufficiently well known in Northeast Russia that it became obvious many years ago that rapid growth in gold mining should primarily be expected from exploration to detect epithermal Au–Ag deposits in volcano-plutonic belts (the OChVB and others). Over 140 tons of gold and 2000 tons of silver have been extracted in the short timespan of 10 years in the unique Kupol Au–Ag epithermal deposit.

The OChVB is the longest among all volcano-plutonic belts in Northeast Russia (over 3000 km) (Fig. 1). Most of the known OChVB Au–Ag epithermal deposits are being mined today. Several deposits have been exhausted: Karamken, Vetvistoe (Magadan Region), Sopka Rudnaya, and Severo-Vostok (Chukotka). A number of deposits (Moroshka, Sentyabr'skoe, Zhil'noe, and Gornoe) are being developed. Most OChVB deposits are of the low-sulfidation type (Kupol, Dvoinoe, Dzhul'etta, and others); the second most numerous group of deposits have intermediate (medium) sulfidation (Dukat, Lunnoe, Gol'tsovoe, and others), while only two deposits (Svetloe and Perekatnoe) can be classified as belonging to the high-sulfidation subtype.

The OChVB was found to contain several tens of promising ore occurrences, over 2000 mineralization sites, and several thousand geochemical anomalies. The mining companies reported extracting 30 tons of Au and over 960 tons Ag from the OChVB epithermal deposits in 2017.

The main goal of the present study is to sum the data, both that available in the literature and new data obtained by these authors, in order to identify geochemical and thermal, pressure, and geochemical features in the Mesozoic OChVB Au–Ag epithermal mineralization, to derive new information concerning the conditions of mineralization, to use the sum of this knowledge in order to design new criteria and refine known ones for assessment of industrial significance and prediction of deposits. The method used in the analytical studies was described in detail in our previous paper (Volkov et al., 2017b).

THE MESOZOIC VOLCANISM AND EPITHERMAL Au–Ag MINERALIZATION IN THE OCHVB

The OChVB is 3000 km long; its average width is 200 km. The OChVB was forming during 25 myr

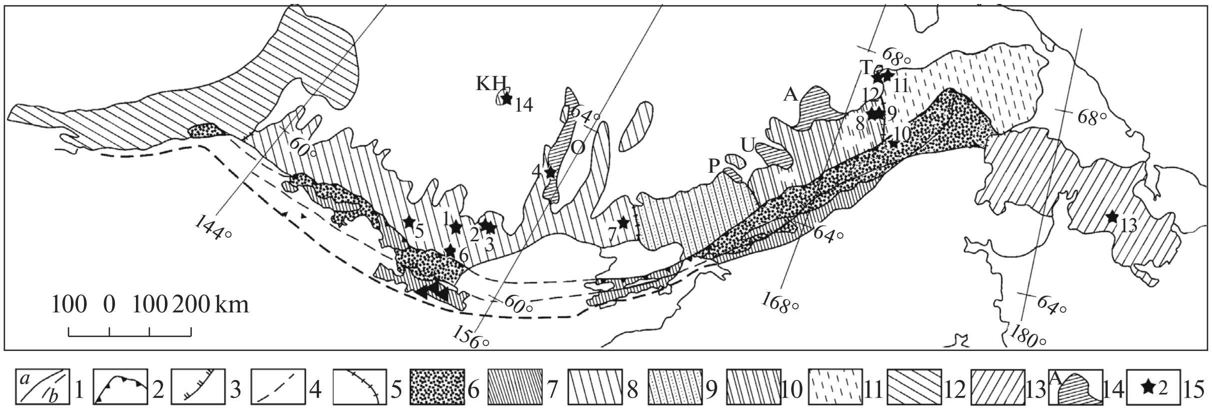

Fig. 1. A map showing the regionalization of the OChVB and the location of the known epithermal Au–Ag deposits. (1) a generalized boundary of the OChVB igneous formations: Albian–Santonian: on land (a) and in sea (b); (2) boundary between the outer and inner zones of the OChVB; (3) boundary of the subzones of depression grabens and of that of magmatogenic uplifts; (4) inferred boundaries in water area; (5) boundaries of sectors in the outer zone and in flank zones; (6) volcanic rocks in outer zone; (7) OChVB magmatogenic uplifts; (8–11) OChVB outer zone, sectors: (8) Okhotsk, (9) Penzhina, (10) Anadyr, (11) Central Chukchi; (12, 13) flank zones: (12) West Okhotsk, (13) East Chukchi); (14) Late orogenic (late Barremian to early Albian) Mesozoic structures: O Omsukchan graben, P Verkhne-Penzhina, U Umkuveem, A Ainakhkurgen, T Tytyl'veem basins, KH Khurchan–Ortukan TMA zone; (15) gold–silver deposits: (1) Nyavlenga, (2) Dzhul'etta, (3) Tikhoe, (4) Dukat, (5) Agan, (6) Oira, (7) Dal'nee, (8) Kupol, (9) Moroshka, (10) Televeem, (10) Dvoinoe, (11) Sentyabr'skoe, (13) Pepenveem, (14) Pechal'noe.

(Belyi, 1994) at the boundary between the continental Verkhoyansk–Chukchi and Koryak–Kamchatka terrane (see Fig. 1). The OChVB evolution proceeded in two phases: (1) the earlier (Albian–Cenomanian) phase in which approximately 90% of all volcanic rocks were produced, and (2) the later (Turonian–Santonian) phase when the Koryak–Kamchatka structures evolved. The formation of the OChVB was probably caused by the Pacific plate being subducted under the collage of the terranes accreted to the Siberian continent. The main sources of acid magma were in the continental crust during this volcanic episode; the crust seems to have been Neoproterozoic (Tikhomirov et al., 2008).

The OChVB consists of three elements (see Fig. 1): the main arcuate part that extends from the lower reaches of the Ul'ya River to the coast of the East Siberian Sea (approximately 2000 km); this part is called the Tauisk–Chaun arcocline, with the other elements being the western Sea-of-Okhotsk and East Chukchi flank zones (Belyi, 1994). In fact, these elements are independent structures that are joined together by a left lateral end-part juncture that were formed during the same span of geologic time.

The outer and flank zones of the OChVB typically contain various isometric negative volcanic structures: subsidence structures with a caldera form (depressions and subsidences) and calderas; circular intrusive–effusive edifices; and volcanic grabens and semi-grabens that have inherited the fault directions in the basement. Dome-like intrusive–effusive and cryptointrusive structures are abundant in all zones, but their role is relatively small, although the mineralization location is not infrequently controlled by these structures.

One important element in the OChVB structure consists in magmatogenic uplifts where the principal parts of the larger intrusive bodies are concentrated. In the inner zone, most of these structures were evolving inheriting the analogous uplifts in the Koni–P'yagin zone of the Taigonos volcanic arc. These were forming in the outer zone during the earlier phase in the OChVB evolution and their relative area is considerably below that in the inner zone. Some of these are elongate parallel to the overall OChVB trend, while others are transverse. Magmatogenic uplifts are infrequent in the flank zones.

The Verkhoyansk–Chukchi Mesozoic features experienced the greatest activation in the late Cretaceous to early Paleogene; the activation seems to have been synchronous with a phase in the OChVB evolution (Sidorov et al., 2013). The area of influence exerted by the Late Mesozoic tectono-magmatic activation (TMA) is identified as a perivolcanic zone of a hazy boundary (as wide as 500 km) that covers the southern part of the Yana–Kolyma system, the Oloi zone, and the Chukchi system. One feature that is noticeable in the deep structure of the perivolcanic zone is the presence of large low-density locations in the lithosphere. These locations are frequently adjacent to the OChVB volcanogenic depressions and basins that show some inheritance of the Mesozoic structural plan. The linear TMA (tectono-magmatic activation) zones are treated here as branches away from the OChVB; chains of volcanic fields and intrusive bodies are also frequently located on extensions of tongues of the belt blanket formations of varying lengths. At the same time, they are different from the belt formations in having different tectono-magmatic features, which are largely controlled by isolated local occurrences of magmatism and by metallogenic features.

All the OChVB structures and the feather TMA zones described above have ore potential. However, the ore potential of volcanogenic structures and of the feather TMA zones are known fragmentarily for the southern part of the Okhotsk sector of the OChVB, for the outer part of the Central Chukchi sector, and very poorly for the inner part of the Anadyr sector.

The complex structure of the basement terranes gave rise to a great diversity of ore assemblages in the OChVB (Sidorov et al., 2009). The inner zone of the belt more frequently contains deposits of the Cu–Mo-porphyry formation containing Au, Ag, and platinoids. The outer and perivolcanic TMA zones typically contain Au–Ag, Ag–base-metal and Sn–Ag mineralization (Sidorov et al., 2011). Epithermal Au–Ag deposits proper (with Au/Ag 1/1–1/10) are more abundant in the outer zone. Silver-dominated deposits (Au/Ag = 1/10–1/1000) are confined to the Omsukchan riftogenic volcanic depression, which introduces complications into the OChVB between the Yana–Kolyma and Omolon terranes (Sidorov et al., 2009). It should also be remarked that the OChVB does not contain any significant Au–Ag–Te deposits and occurrences, which were thought by Nolan (1933) to be related to small volcanic bodies in the Cenozoic volcanic belts of the western United States.

The generation of epithermal deposits of dominantly Ag and Au–Ag types in the volcanic belts is largely due to the fact that they are underlain by potentially gold- and silver-bearing rock sequences of the Verkhoyansk and Chukchi terrigenous units, as well as by older metamorphic units of median massifs (cratons), which were extra sources of metals for volcanogenic–plutonogenic deposits (Volkov et al., 2006).

Comparison among different OChVB sectors by the intensity of epithermal mineralization shows that the well-known Okhotsk sector (the Karamken, Nyavlenga, Dzhul'etta, and Dukat deposits, the Evensk group, etc.) is inferior to the poorly known Anadyr sector in terms of proved Au reserves in epithermal deposits. The Anadyr deposits are Kupol, Moroshka, Sentyabr'skoe, Valunistyi, and Dvoinoi.

This fact seems to be due to the rather complex geological structure of the Okhotsk sector. In this sector one finds abundant rejuvenated epithermal deposits (Goncharov and Sidorov, 1979). In addition, the Okhotsk sector is dominated by acidic igneous units of the Ag–Sn–Mo type (Sidorov et al., 2009). At the same time, one discerns a pronounced relationship between epithermal Au–Ag mineralization and the Cu-porphyric ore-forming system on the Kupol deposit in the Anadyr sector (Volkov et al., 2012).

The geochemical features of Au–Ag ores in epithermal deposits that will be discussed below show many similarities to the ore assemblage patterns pointed out above.

THE GEOCHEMICAL FEATURES OF THE OCHVB EPITHERMAL ORES

The ores sampled from the Mesozoic epithermal Au–Ag deposits are dominated by SiO_2 (67.6–92.8%) along with noticeable concentrations of Al_2O_3 (3.2–14.0%), K_2O (0.44–5.5), and Fe_2O_3 (0.48–5.1) (Table 1). The ores of the Tikhoe deposit are found to contain noticeable concentrations of Na_2O (2.27%) and CaO (4.83%) (see Table 1), which is caused by mineralization in an argillite zone (Volkov et al., 2015). The Dukat ores typically show high concentrations of MnO (3.9) and the Nyavlenga ores have high concentrations of MgO (3.46) (see Table 1), which is due to the special type of mineralization in these deposits (Volkov et al., 2014). The metasomatic ores of the Agan deposit (Volkov et al., 2015) show the highest total $Na_2O + K_2O$ (see Table 1). Judging from the data in this table, the concentration of sulfides in the ore samples studied here varies in a wide range (S_{total} is between 0.3% and 3.2%).

The results of trace-element analyses for the OChVB ores of volcanogenic epithermal Au–Ag deposits and host rocks are presented in Table 2 and in Fig. 2 where the values have been normalized by the means for the upper crust (Taylor and McLennan, 1985). It follows from Table 2 and Fig. 2 that the ores are clearly enriched in a wide range of elements (Li, P, Rb, V, Cr, Sc, Ba, Mn, Au, Ag, As, Sb, Te, Cu, Mo, Zn, Pb, In, Cd, Ga, Co, Mo, Bi, Tl, Cs, Be, Se, W, and U) compared with the upper crustal means (Tayler and McLennan, 1985). The enrichment ratios vary between a few times (Li, P, Sc, Rb, Cs, Cr, V, Tl, Ba, Se, W, and U) and a few tens (Mo, Mn, and Sn), hundreds (Pb, Cu, Zn, Be, and Te), and thousands (As, Sb, In, Cd, and Bi), reaching a few tens or hundreds of thousands of times (Au and Ag), thus providing evidence of a geochemical affinity of trace elements and their synchronous participation in the mineralization.

Comparative analysis of mean trace-element concentrations in the ores of the OChVB epithermal Au–Ag deposits shows great similarities in composition and distribution (see Table 2, Fig. 2). This shows that the mineralization of these deposits occurred under similar conditions. At the same time, the Dukat ores are characterized by an appreciable synchronous enrichment in Be and Mn (see Fig. 2), which is due to a wide abundance in the ores of minerals that contain these admixtures (Konstantinov et al., 1998). The Pechal'noe ores show an obvious synchronous enrichment in Li, Be, Rb, Cs, Mo, W, and Tl, which corresponds with the composition of the host volcanic rocks (Egorov et al., 2005; Volkov et al., 2017b). The

Table 1. The silicate composition of ore samples (wt %) from OChVB epithermal Au–Ag deposits

Components, %	DEPOSITS													
	Dvoinoi	Dzhul'etta	Dukat	Kupol	Moroshka	Oira	Dal'nee	Pechal'noe	Tikhoe	Nyavlenga	Sentyabr'skoe	Pepenveem	Televeem	Agan
n	6	6	5	6	5	6	4	6	5	7	6	5	2	5
SiO_2	87.015	84.17	75.186	92.838	80.788	75.023	76.94	85.923	76.834	67.589	68.267	93.254	82.48	84.41
TiO_2	0.057	0.03	0.046	0.118	0.098	0.153	0.328	0.255	0.224	0.487	0.28	0.046	0.07	0.07
Al_2O_3	5.788	4.463	6.06	3.845	6.552	7.928	10.898	7.17	6.228	14	9.618	2.754	7.71	7.92
Fe_2O_{3total}	0.487	2.44	5.122	0.645	2.818	2.053	5.023	2.232	2.91	5.159	4.538	1.794	1.345	1.03
MnO	0.039	0.049	3.925	0.107	0.112	0.063	0.113	0.022	0.126	0.082	0.104	0.013	0.01	0.01
MgO	1.203	0.293	1.08	0.535	1.482	2.085	1.253	0.392	1.534	1.241	3.468	0.084	0.12	<0.10
CaO	0.758	0.613	1.044	0.785	3.134	0.94	0.39	0.072	7.736	4.83	2.417	<0.10	<0.10	0.06
Na_2O	0.128	0.142	0.306	0.048	0.078	0.635	0.328	0.145	0.348	2.277	0.433	0.052	0.16	0.33
K_2O	3.615	2.682	1.97	0.442	2.304	3.35	3.24	2.858	1.406	3.647	2.88	0.812	5.57	5.51
P_2O_5	0.022	0.015	0.008	0.027	0.02	0.057	0.1	0.103	0.072	0.214	0.082	0.028	0.02	0.03
S_{total}	0.303	3.21	0.746	0.418	1.326	0.273	1.243	0.542	1.248	0.421	2.987	0.356	1.315	0.56
L.O.I.	–	–	–	0.923	2.052	0.99	–	–	–	1.226	0.378	–	–	–
Σ	99.415	98.107	95.493	100.731	100.764	93.55	99.856	99.714	98.666	101.173	95.452	99.193	98.8	99.93

X-ray fluorescence analysis, at IGEM RAN laboratory, Analyst A.I. Yakushev; L.O.I. is short for loss on ignition; here and below *n* denotes the number of samples.

Table 2. The element composition (g/t) of ore samples from the OChVB epithermal Au–Ag deposits

Elements, g/t	DEPOSITS												
	Dvoinoe	Dzhul'etta	Dukat	Kupol	Moroshka	Oira	Dal'nee	Pechal'noe	Tikhoe	Nyavlenga	Sentyabr'skoe	Pepenveem	Televeem	Agan
Li	77.333	51.333	67	108.667	111.4	57.333	40.5	152.047	67.096	25.9	58.5	178.056	48.108	104.200
Be	0.825	0.727	525.96	0.902	0.766	0.617	1.098	21.773	0.441	1.424	0.585	1.45	4.569	0.952
P	1587.5	n.d.	n.d.	833.667	743.8	396.333	394.75	n.d.	n.d.	583.429	339.333	n.d.	n.d.	3.800
Sc	4.688	n.d.	n.d.	19.985	4.04	1.75	12.2	1.687	4.073	10.757	9.333	n.d.	11.823	10.840
Ti	235.317	78.167	124.2	652.5	491.56	844.833	1689.75	1339.038	982.965	2711.286	1406.067	149.345	343.755	299.600
V	6.367	2.288	0.81	30.167	21.4	6.217	80.75	20.06	28.536	103.814	65.167	1.949	17.619	5.400
Cr	20.35	9.633	6.32	35.5	8.58	8.783	33.25	50.386	18.299	22.4	36	12.157	9.548	13.820
Mn	228.833	367.5	29268.2	818.333	846.2	464	793.75	113.516	835.989	585.143	737.833	44.968	42.678	58.000
Co	1.108	1.185	1.04	5.328	2.66	1.205	14.2	1.977	3.193	9.561	8.467	0.714	0.506	0.145
Ni	1.247	0.692	0.112	3.083	1.648	0.335	2.325	8.701	4.057	5.7	3.583	1.223	2.113	2.224
Zn	363.5	1868.217	3183	63	1390	314.667	130.75	59.599	4645.216	51	16690.333	11.943	248.27	8.600
Ga	4.067	1.597	15.6	5.45	4.72	7.617	26.75	18.635	6.207	29.857	26.7	3.809	8.324	8.420
As	75.5	218.8	13.334	206.667	1336.4	17.1	127.25	1856.159	14.416	10.843	71.5	1281.173	318.184	12.220
Se	7.333	68.033	55.6	29.667	n.d.	1.667	25.975	13.088	206.812	2.223	6.367	n.d.	48.623	7.860
Rb	152.167	46.383	62.8	18.417	59.2	93.5	104.75	217.19	46.188	115.429	93.283	25.582	243.508	166.000
Sr	44.333	34.5	4.114	31.85	57.8	80.833	169.5	25.929	133.539	251.429	115	21.144	84.575	21.600
Y	1.47	0.942	6.16	5.958	4.76	5.833	10.55	6.118	5.433	11.814	6.035	2.687	1.926	11.760
Zr	13.043	4.972	11.32	23.11	17.426	44.867	51	44.386	37.018	62	55.925	12.158	16.016	47.740
Nb	0.342	0.033	0.688	0.883	0.54	1.135	2.635	3.341	1.276	8.629	2.82	0.545	1.449	2.060
Mo	0.404	0.005	0.088	8.695	41.32	0.823	2.225	4.44	0.16	8.371	1.129	10.438	43.768	2.440
Ag	79.667	516.667	256.5	154	155.6	40.733	189	106.698	52.768	1.629	41.5	207.777	1077.053	210.220
Cd	3.983	5.949	12.064	0.215	31.026	22.612	0.37	0.144	8.314	0.251	223	0.191	0.998	0.051
In	n.d.	0.015	n.d.	108.417	n.d.	0.015	1.425	28.737	336.427	2.813	0.872	0.497	0.3	0.161
Sn	0.978	0.27	2.508	1.373	2.1	1.612	0.818	0.647	1.075	1.577	1.395	2.121	3.558	60.200
Sb	106.667	265.967	42.58	395.333	157	5.235	65.25	81.248	2.988	1.373	24.5	45.736	231.698	35.746
Te	5.95	10.722	0.022	0.235	8.976	7.627	12.188	0.279	521.99	0.075	3.95	0.297	72.186	4.786
Cs	8.233	0.585	3.14	5.4	9.54	3.733	4.6	21.176	2.263	5.61	13.033	3.512	4.729	1.940
Ba	101	1738.167	160.6	27	187.6	224.167	416.5	147.48	119.55	348.857	421.5	151.308	216.842	350.600
La	1.379	0.73	2.888	3.798	3.626	3.507	10.725	8.231	6.429	11.886	7.552	5.941	4.426	8.600

Table 2. (Contd.)

Elements, g/t	DEPOSITS													
	Dvoinoe	Dzhul'etta	Dukat	Kupol	Moroshka	Oira	Dal'nee	Pechal'noe	Tikhoe	Nyavlenga	Sentyabr'skoe	Pepenveem	Televeem	Agan
Ce	3.21	1.64	6.592	6.75	6.98	8.462	22.225	16.379	12.729	24.143	14.738	11.561	8.126	16.280
Pr	0.373	0.188	0.824	0.747	0.892	1.193	2.775	1.996	1.525	3.129	1.912	1.344	0.877	1.954
Nd	1.528	0.822	3.444	2.835	3.4	5.267	11.225	7.291	5.735	12.529	7.513	4.87	2.93	8.140
Sm	0.3	0.178	0.85	0.635	0.78	1.248	2.208	1.482	1.147	2.429	1.364	1.026	0.541	1.630
Eu	0.059	0.171	0.105	0.253	0.378	0.338	0.7	0.311	0.727	0.799	0.422	0.159	0.145	0.322
Gd	0.39	0.237	0.89	0.611	0.912	1.25	2.158	1.17	1.265	2.357	1.181	0.896	0.301	1.592
Tb	0.034	0.017	0.151	0.136	0.129	0.187	0.358	0.196	0.167	0.356	0.188	0.132	0.054	0.284
Dy	0.243	0.153	1.037	0.838	0.872	1.185	1.923	1.105	0.971	2.057	1.065	0.711	0.346	1.820
Ho	0.037	0.022	0.202	0.187	0.143	0.23	0.37	0.237	0.189	0.411	0.22	0.114	0.065	0.356
Er	0.139	0.071	0.616	0.503	0.382	0.72	0.978	0.703	0.551	1.15	0.627	0.266	0.218	1.024
Tm	0.01	0.002	0.077	0.061	0.048	0.094	0.142	0.103	0.071	0.168	0.093	0.033	0.031	0.130
Yb	0.149	0.068	0.606	0.449	0.372	0.719	0.808	0.689	0.485	1.093	0.63	0.212	0.261	0.988
Lu	0.01	0.001	0.072	0.073	0.044	0.098	0.122	0.096	0.065	0.161	0.093	0.031	0.044	0.132
Hf	0.184	0.004	0.308	0.733	0.44	1.127	1.37	1.244	0.858	1.8	1.552	0.005	0.448	1.194
Ta	0.009	n.d.	0.032	0.112	0.026	0.075	0.145	0.184	0.083	0.487	0.217	0.038	0.088	0.111
W	0.202	0.147	0.203	12.3	0.88	0.707	2.15	17.861	0.029	1.613	1.687	3.616	n.d.	0.106
Tl	1.977	0.387	1.222	1.453	1.414	1.678	1.038	6.86	3.995	1.824	1.017	0.192	3.106	3.830
Pb	438.667	11389.167	3479	75.483	1038.2	305.5	16.75	13.534	5582.222	26.629	25243.167	2570.633	374.958	27.940
Bi	0.54	0.125	0.167	0.034	0.18	0.112	1.304	0.798	0.188	0.27	0.077	152.29	0.468	0.205
Th	1.043	0.125	1.14	0.962	0.427	1.233	1.025	2.162	1.877	3.129	4.143	2.134	1.756	2.480
U	0.544	0.067	0.469	0.499	0.305	0.51	0.324	0.702	0.549	1.171	1.021	1.44	0.74	3.732
Au	51.218	1805.721	32.132	67.965	84.434	25.937	360.349	2.919	1714.051	7.449	461.729	1.377	158.005	3.202
Cu	328.333	768.333	1424	33.333	226	138.333	82.5	15.318	632.084	30	2096.667	43.844	6587.089	4.000
n	6	6	5	6	5	6	4	6	5	7	6	5	2	5

Inductively coupled plasma mass spectroscopy (ICP-MS), IGEM RAN laboratory (Analyst Ya.V. Bychkova). Gold in the samples was determined by atomic absorption spectroscopy with electrothermal atomization using a Spectr AA220 Z spectrometer (Analyst V.A. Sychkova); n.d. means not detected.

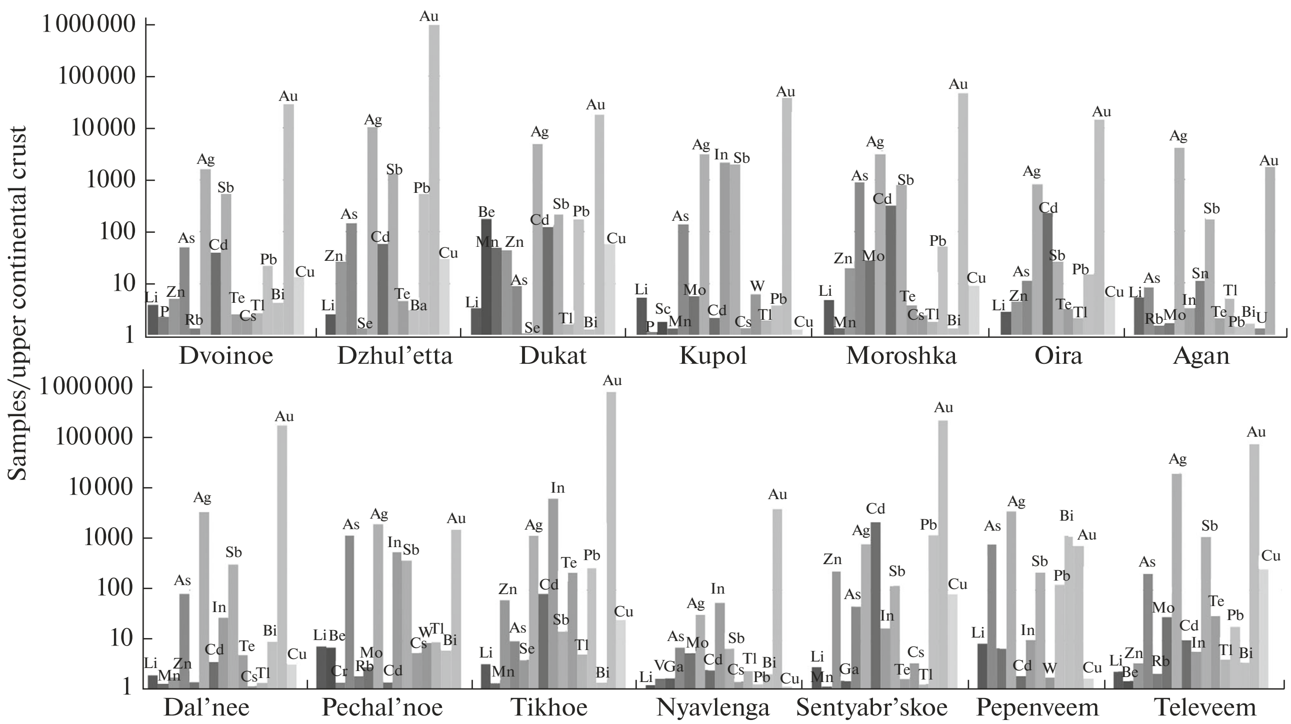

Fig. 2. Trace elements in the ores of the OChVB epithermal Au–Ag deposits as normalized by the mean upper crustal values (Taylor and McLennan, 1985).

epithermal ores in the Agan deposit have a distinguishing feature, viz., a high enrichment in Sn (see Fig. 2), which classifies the ores as belonging to the tin-porphyritic mineralizing system (Volkov et al., 2015). Similar distributions but different intensities of individual elements occur in the Kupol, Moroshka, Dvoinoi, Sentyabr'skoe, Televeem, Dzhul'etta, Oira, Dal'nee, Nyavlenga, and Tikhoe deposits (see Fig. 2), which may have been because they belong to the Cu–Mo-porphyritic mineralizing system (Volkov et al., 2012, 2014). The low intensity of elements in the distribution of the Nyavlenga deposit compared with the ores of the other known deposits seems to be due to thermal metamorphism of the ores (Savva et al., 2007). The noticeable enrichment in Bi and W observed in the Pepenveem ores provides evidence that this deposit belongs to a mineralizing system related to granitoid intrusions (Lang et al., 2000).

Comparative analysis of the trace-element distributions in the ores over gold concentration class (Fig. 3) emphasizes a synchronous enrichment of the ores in a similar set of trace elements from low (1–5 g/t) to high class (>100 g/t).

The OChVB host volcanic rocks are also enriched in a wide range of elements (Li, Sc, Ti, V, Mn, Sr, Co, Ba, REEs, etc.) compared with the upper crustal values (Taylor and McLennan, 1985), but the enrichment ratios for most of them are low (2 to 5 times). The highest enrichment ratios ranging between 5 and 10 or higher (As, Ag, Pb, Sb, and Mo) were found for host rocks within the epithermal ore fields (Sakhno et al., 2015; Kravtsova, 2010).

According to V.A. Zharikov et al. (1999), light REEs pass into aqueous fluid as the pressure increases, while heavy ones are retained in the magma, so that one can treat the former as "hydrophile" elements and the latter as "magmaphile" ones. Three REE sets can be identified (Mineev, 1974): the cerium set (La, Ce, Pr, and Nd), the yttrium set (Sm, Eu, Gd, Dy, and Ho), and the scandium set (Er, Yb, and Lu). Judging from the data in Table 3, the REE distributions of the ores are dominated by light "hydrophile" lanthanoids of the "cerium" set. A similar REE composition is also typical of the OChVB host volcanic rocks (Kravtsova et al., 2005; Kravtsova and Almaz, 2006; Kravtsova, 2010; Tikhomirov et al., 2008, 2016; Sakhno et al., 2015).

We know that Cl-bearing hydrothermal fluids can effectively concentrate light REEs, but are depleted in heavy REEs (Oreskes and Einaudi, 1990); in that case the Hf/Sm, Nb/La, and Th/La ratios in the ores are generally below 1, while F-rich fluids synchronously concentrate light and heavy REEs, since the Hf/Sm, Nb/La, and Th/La ratios are usually greater than 1 (Oreskes and Einaudi, 1990). The ores in most of the OChVB epithermal Au–Ag deposits are evidently enriched in light REEs and depleted in heavy REEs, and have Hf/Sm, Nb/La, and Th/La ratios below 1 (see Table 3); one exception is the Sentyabr'skoe deposit where Hf/Sm = 1.13. It follows that the ore-

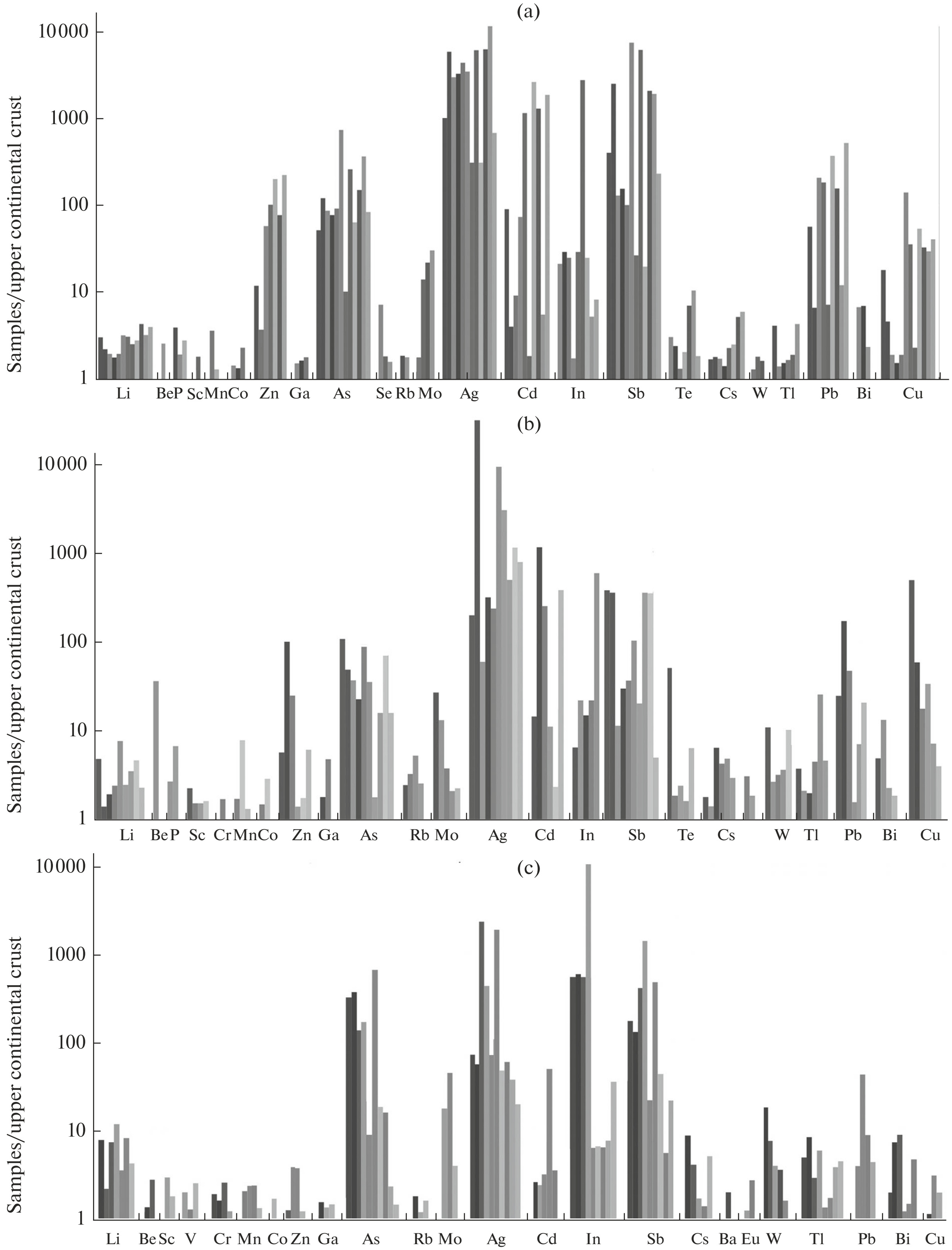

Fig. 3. The trace-element distribution over classes of Au concentration in the ores of the OChVB epithermal Au–Ag deposits as normalized by the mean upper crustal values (Taylor and McLennan, 1985). Classes of Au concentration (g/t): >100 (a), 10–20 (b), and 1–5 (c).

Table 3. The indicator parameters of ore sampled from the OChVB epithermal Au–Ag deposits

Indicators	DEPOSITS													
	Dvoinoe	Dzhul'etta	Dukat	Kupol	Moroshka	Oira	Dal'nee	Pechal'noe	Tikhoe	Nyavlenga	Sentyabr'skoe	Pepenveem	Televeem	Agan
∑REE	7.861	4.3	18.355	17.873	18.958	24.497	56.714	39.99	32.057	62.666	37.598	27.296	18.365	43.252
∑LREE	6.848	3.73	14.703	15.018	16.056	20.014	49.858	35.691	28.293	54.913	33.501	24.901	17.045	36.926
∑HREE	1.013	0.57	3.652	2.855	2.902	4.483	6.857	4.3	3.764	7.753	4.097	2.396	1.32	6.326
∑LREE/∑HREE	6.761	6.541	4.026	5.26	5.533	4.465	7.272	8.3	7.517	7.083	8.178	10.395	12.911	5.837
Hf/Sm	0.613	0.021	0.362	1.156	0.564	0.903	0.621	0.839	0.747	0.741	1.137	0.005	0.828	0.733
Nb/La	0.248	0.046	0.238	0.233	0.149	0.324	0.246	0.406	0.198	0.726	0.373	0.092	0.327	0.240
Th/La	0.757	0.171	0.395	0.253	0.118	0.352	0.096	0.263	0.292	0.263	0.549	0.359	0.397	0.288
Y/Ho	39.91	42.481	30.495	31.891	33.38	25.399	28.514	25.789	28.81	28.715	27.473	23.538	29.777	33.034
U/Th	0.521	0.537	0.411	0.519	0.715	0.414	0.316	0.325	0.293	0.374	0.247	0.675	0.422	1.505
Rb/Sr	3.432	1.344	15.265	0.578	1.024	1.157	0.618	8.376	0.346	0.459	0.811	1.21	2.879	7.685
Sr/Ba	0.439	0.02	0.026	1.18	0.308	0.361	0.407	0.176	1.117	0.721	0.273	0.14	0.39	0.062
Zr/Hf	70.952	1355.909	36.753	31.514	39.605	39.822	37.226	35.688	43.169	34.444	36.042	2382.513	35.747	39.983
Nb/Ta	37.273	–	21.5	7.899	20.769	15.133	18.141	18.173	15.292	17.713	12.986	14.211	16.475	18.559
Co/Ni	0.889	1.713	9.286	1.728	1.614	3.597	6.108	0.227	0.787	1.677	2.363	0.584	0.24	0.065
Te/Se	0.811	0.158	0	0.008	–	4.576	0.469	0.021	2.524	0.034	0.62	–	1.485	0.609
Au/Ag	0.643	3.495	0.125	0.441	0.543	0.637	1.907	0.027	32.483	4.574	11.126	0.007	0.147	0.015
Eu/Eu*	0.773	2.635	0.488	1.12	1.382	0.916	1.011	0.779	1.746	1.066	1.033	0.627	1.004	0.696
Ce/Ce*	1.15	1.089	1.071	0.909	0.952	1.089	1.032	1.009	1.005	1.012	0.989	0.992	0.97	0.953
LaN/YbN	6.271	7.314	3.237	5.753	6.625	3.313	9.023	8.111	8.998	7.388	8.143	18.994	L11.517	5.913
LaN/SmN	2.871	2.557	2.122	3.738	2.903	1.754	3.034	3.468	3.499	3.056	3.457	3.617	5.11	3.295
GdN/YbN	2.114	2.827	1.189	1.101	1.985	1.407	2.162	1.372	2.108	1.745	1.517	3.413	0.933	1.304
LaN/LuN	14.074	90.968	4.152	5.413	8.593	3.708	9.125	8.855	10.225	7.656	8.428	20.179	10.502	6.763
∑Ce	6.489	3.381	13.748	14.13	14.898	18.428	46.95	33.898	26.418	51.686	31.715	23.716	16.359	34.974
∑Y	1.063	0.778	3.236	2.659	3.214	4.438	7.715	4.501	4.466	8.409	4.44	3.038	1.452	6.004
∑Sc	0.298	0.139	1.294	1.024	0.798	1.537	1.907	1.488	1.101	2.404	1.35	0.509	0.523	2.144
Eu/Sm	0.197	0.956	0.124	0.399	0.485	0.271	0.317	0.209	0.634	0.329	0.309	0.155	0.268	0.197
Ce/Yb	21.496	24.177	10.878	15.05	18.774	11.769	27.523	23.757	26.227	22.092	23.394	54.412	31.127	16.478
Eu/Ce	0.018	0.104	0.016	0.038	0.054	0.04	0.031	0.019	0.057	0.033	0.029	0.014	0.018	0.020

$Eu/Eu^* = Eu_N/(Sm^*_N(Tb^*_N Eu_N)^{1/2})^{1/2}$; $Ce/Ce^* = Ce_N/((2La_N + Sm_N)/3)$, REE , LREE stands for light REE, HREE for heavy REE.

forming fluids of the deposits belonged to a NaCl–H_2O hydrothermal system that was enriched in Cl relative to F; this agrees with studies of fluid inclusions in ore quartz (Volkov et al., 2012; Kolova et al., 2015; Prokof'ev et al., 2015, among others).

The U/Th ratio for an ore reflects the redox conditions of the host rocks (Jones and Manning, 1994): U/Th $\leq$ 0.75 occurs in an oxidizing environment; U/Th 0/75–1.25 is characteristic of an environment without oxygen, and U/Th > 1.25 for a reducing environment. Judging from the data in Table 3, the U/Th ratios in the ores of the deposits studied here are below 0.75 (they vary between 0.24 and 0.71), providing evidence of an oxidizing environment during their mineralization (Jones and Manning, 1994). The high values of that ratio (1.5) in the Agan ores (see Table 3) indicate a reducing environment of mineralization that is characteristic for the shallow level of the epithermal system where the deposit was formed (Volkov et al., 2015).

The Co/Ni ratios in the Dvoinoe, Pechal'noe, Tikhoe, Pepenveem, Televeem, and Agan ores (see Table 3) are considerably below 1.0 (they vary between 0.06 and 0.88), which is characteristic for medium- and low-temperature hydrothermal fluids of meteoric origin (Kun et al., 2014). Values above 1.5 in the Dzhul'etta, Dukat, Kupol, Moroshka and other ores (see Table 3) provide evidence of an obvious role played by a magmatic fluid in the mineralization (Kun et al., 2014). The high Co/Ni ratio in the ores shows the superposition of a later magmatic fluid on the earlier mineralization and is a consequence of a rejuvenated mineralization (Goncharov and Sidorov, 1979).

Effective use of the Y/Ho ratio for assessing the origin of mineralizing fluids was shown in (Bau, 1991; Jones and Manning, 1994; Monecke et al., 2002). According to Table 3, the Y/Ho ratios in the OChVB epithermal Au–Ag ores studied here vary between 23.53 and 42.48, which corresponds with the range of the ratios that are characteristic of the present-day hydrothermal fluids in backarc basins (Bau, 1991; Jones and Manning, 1994; Monecke et al., 2002).

The REE composition in the OChVB epithermal Au–Ag ores studied here is shown in Table 2, while the chondrite-normalized REE distributions are plotted in Fig. 4. Abnormally low values of ΣREE (between 4.3 and 18.95 g/t) were found in the Dvoinoe, Dzhul'etta, Dukat, Kupol, Moroshka, and Televeem ores (see Table 3). Lower values of ΣREE (24.49–39.99 g/t) are characteristic for typical epithermal ores in the Oira, Pechal'noe, Tikhoe, Pepenveem, and Sentyabr'skoe deposits. Higher values (43.25–62.66) of ΣREE were found in the Agan, Nyavlenga, and Dal'nee ores. Low total REE concentrations, the same as in the OChVB deposits, were found in productive quartz in the ores of the epithermal deposits on the Kuramin Range, Uzbekistan and of the Banská Štiavnica area, Slovakia (Vinokurov et al., 1999). The total REE concentration in the epithermal Au–Ag ores of the deposits studied here (see Table 3) is appreciably lower than those in the OChVB igneous and volcanic rocks and in island-arc andesites (Kravtsova et al., 2005; Kravtsova and Almaz, 2006; Kravtsova, 2010; Tikhomirov et al., 2008, 2016).

The chondrite-normalized REEs of the ores studied here make slightly dipping near-chondrite distributions (see Fig. 4a) that exhibit many similarities in their configurations to those of the REE distributions for the OChVB rocks (see Fig. 4c), as well as for island-arc andesites (Kravtsova et al., 2005; Kravtsova and Almaz, 2006; Kravtsova, 2010, among others).

The REE distributions clearly distinguish three sets of ore (see Fig. 4a). The distributions of the first set (Dzhul'etta, Moroshka, Tikhoe, and Kupol) show well-pronounced Eu maxima (see Figs. 4a, 5). Pronounced Eu minima were found for the distributions of the Dvoinoe, Dukat, Pepenveem, and Agan ores (see Figs. 4a, 5). The slightly dipping near-chondrite distributions that involve no pronounced Eu maxima and minima are characteristic for the ores of the third set (Nyavlenga, Televeem, Pechal'noe, Oira, and Sentyabr'skoe). Differently directed distributions were found for the Kupol ores (see Fig. 5), which supports the identification of two types, viz., high- and low-sulfidation epithermal mineralization, on this deposit (Volkov et al., 2012).

The REE distributions clearly separate the OChVB host volcanic rocks into two sets. Acidic rocks typically show distributions with pronounced Eu minima, while intermediate rocks make slightly dipping near-chondrite distributions. We note that the epithermal Au–Ag Cenozoic deposits of Kamchatka that are localized in intermediate (andesitic to dacitic) rocks were found to have near-chondrite REE distribution configurations (Takahashi et al., 2007; Andreeva, 2013).

To summarize, we can state that the different ratios in the ore-containing section that is composed of volcanic rocks with different compositions seems to control the REE distribution configurations in the ores. These results suggest that the OChVB host rocks, as well as the host rocks in the other volcano-plutonic belts in Northeast Russia (Volkov et al., 2017a) might be the source of the REEs and possibly of other trace elements for the ore-forming fluids.

According to S.V. Vinokurov et al. (1999), positive Eu anomalies constitute a characteristic feature of productive quartz in epithermal Au–Ag deposits, while oreless quartz in such deposits exhibits negative Eu anomalies (Vinokurov et al., 1999). This inference is also supported by our results (see Fig. 4b). Judging from this figure, the distributions of rich ores differ from those of poor ores in having pronounced Eu maxima. It may be hypothesized that the Eu maxima in the ores of the first set (see Fig. 4a) are due to their richness.

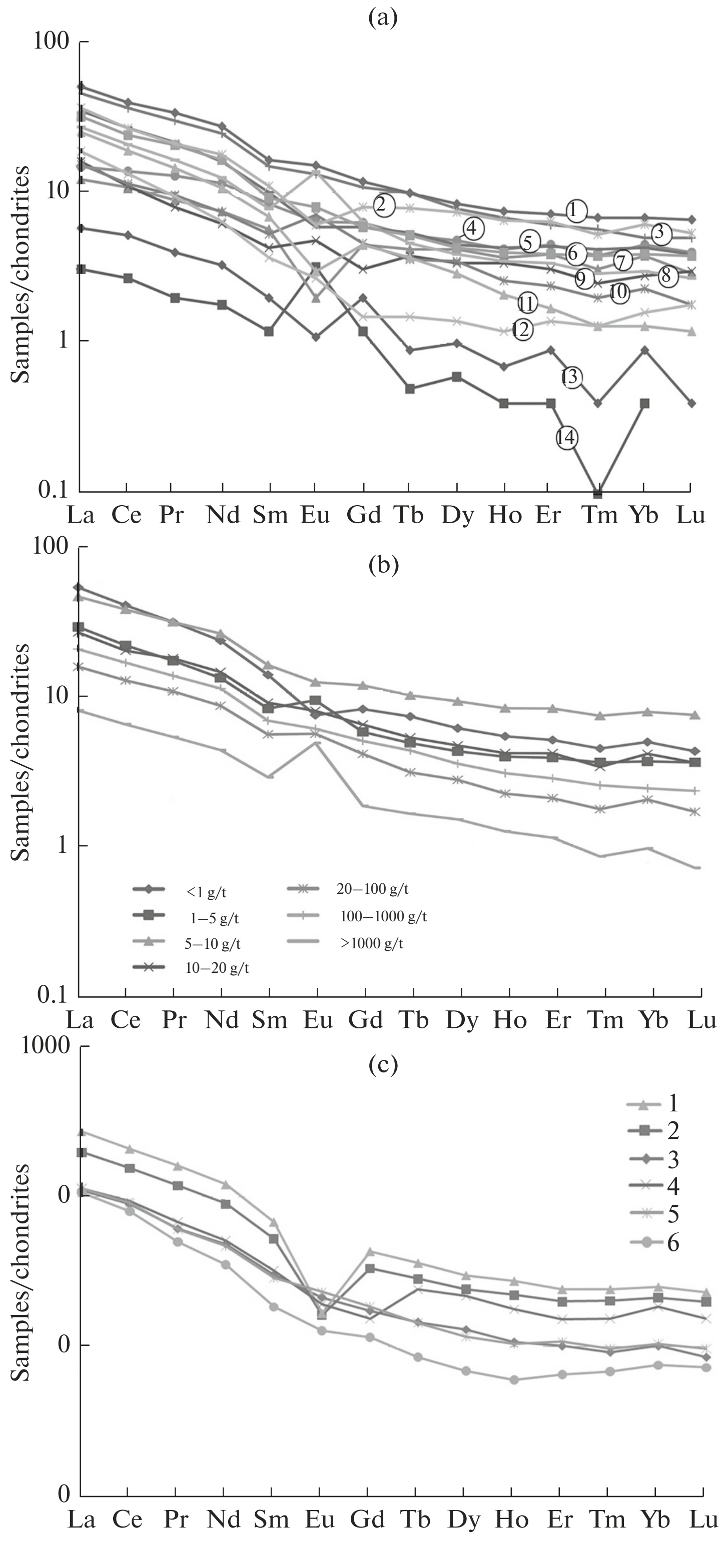

Fig. 4. The distribution of chondrite-normalized mean REE values ((a) over deposits, (b) over classes of Au concentration) in the ores of epithermal Au–Ag deposits and host rocks (c) in the OChVB. Numerals in circles (1–14) refer to known deposits: (1) Nyavlenga, (2) Dal'nee, (3) Agan, (4) Pechal'noe, (5) Oira, (6) Sentyabr'skoe, (7) Dukat, (8) Tikhoe, (9) Kupol, (10) Moroshka, (11) Pepenveem, (12) Televeem, (13) Dvoinoe, (14) Dzhul'etta. OChVB rocks: (1) rhyolite lavas; (2) rhyolite ignimbrites; (3) andesites; (4) dacites; (5) dacitic tuffs; (6) rhyolite dikes (Tikhomirov et al., 2008; Sakhno et al., 2015).

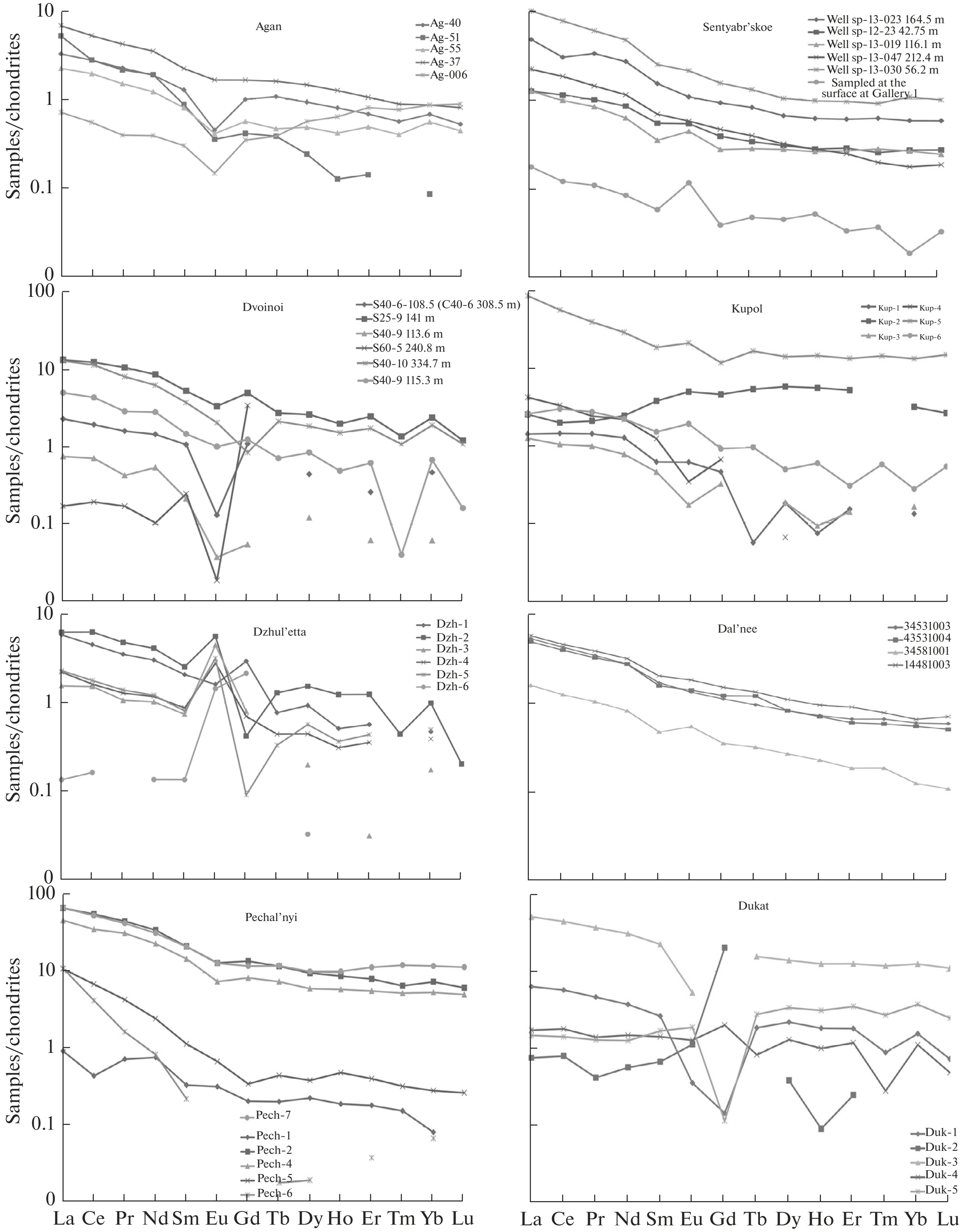

Fig. 5. The chondrite-normalized REE distribution in the ores of the OChVB epithermal Au–Ag deposits. Ag.37 etc. are sample numbers.

Table 4. The physico-chemical parameters of mineral-forming fluids at the OChVB Au–Ag deposits

Deposit	Physico-chemical parameters of fluids				References
	T, °C	C, wt %	d, g/cm^3	P, bars	
Dukat	201–357 (6)	2.5–2.8	0.63–0.88	90 (1)	Berman et al., 1993
Dal'nee	220–355 (22)	0.6–2.4	0.57–0.86	–	Kravtsova, 2010
Dukat	185–435 (46)	1.5–37.0	0.64–1.11	–	Kravtsova, 2010
Kupol	222–267 (4)	2.1	0.78–0.86	–	Volkov et al., 2006
Kupol	225 (1)	1.9	0.85	–	Sidorov et al., 2007
Kupol	222–276 (12)	0.5–3.2	0.75–0.86	–	Volkov et al., 2012
Dvoinoe	154–251 (7)	0.2–5.0	0.80–0.95	–	Volkov et al., 2012
Arykvaam	234–267 (10)	0.4–1.2	0.79–0.82	–	Volkov et al., 2012
Kupol	224–276 (12)	0.5–3.2	0.75–0.86	–	Prokof'ev et al., 2012
Dvoinoe	154–251 (7)	0.2–5.0	0.80–0.95	–	Prokof'ev et al., 2012
Dvoinoe	133–254 (9)	0.5–3.9	0.82–0.94	–	Nikolaev et al., 2013
Sentyabr'skoe	155–360 (32)	0.9–8.1	0.24–0.94	80–570 (8)	Nikolaev et al., 2013
Nyavlenga	157–359 (27)	0.3–8.2	0.56–0.93	–	Volkov et al., 2014
Dzhul'etta	126–222 (20)	1.2–5.6	0.86–0.97	–	Prokof'ev et al., 2015
Tikhoe	105–260 (11)	1.0–9.2	0.82–1.01	–	Kolova et al., 2015
Sentyabr'skoe	137–296 (34)	0.0–7.4	0.69–0.96	–	Savva et al., 2016

The number of determinations is enclosed in parentheses, a dash means no data.

Eu and Ce anomalies are commonly treated as marking the redox potential of a mineralization environment (Bortnikov et al., 2007; Goryachev et al., 2008; Jones and Manning, 1994). The ores sampled from the OChVB deposits (see Table 3) show δCe and δEu varying between negative or weakly negative and moderately positive values (δCe = between 0.90 and 1.15) and (δEu = between 0.48 and 2.63). This combination of δCe and δEu indicates low-oxidation and oxidation conditions that existed during the deposition of the OChVB epithermal ores. The low Eu/Sm ratios (<1) in the ores studied here (see Table 3) suggest the inference that the OChVB mineralization occurred in the upper crust under similar physical and chemical conditions (Vinokurov, 1996).

Comparison between the data obtained here and known published examples (Vinokurov et al., 1999; Kravtsova, 2010, among others) indicates that the patterns identified here, viz., the depletion of ores in rare-earth elements, the prevalence of light lanthanoids over heavy ones, low Eu/Sm ratios (<1), and positive Eu anomalies, all constitute, in all probability, typical features for the epithermal mineralization system.

THE DISTINGUISHING FEATURES OF THE ORE-FORMING FLUIDS

Many results have been reported concerning physico-chemical parameters and composition of ore-forming fluids for the OChVB Au–Ag deposits (Table 4, Fig. 6). Papers exist concerning the conditions of mineralization for the Dukat (Goncharov and Sidorov, 1979; Berman et al., 1993; Kravtsova et al., 2003; Konstantinov et al., 1998, among others), Dal'nee (Kravtsova et al., 2003; Kravtsova, 2010), Kupol (Volkov et al., 2006, 2012; Sidorov et al., 2007; Prokof'ev et al., 2012), Dvoinoe (Volkov et al., 2012; Prokof'ev et al., 2012; Nikolaev et al., 2013; Kolova et al., 2018), Arykvaam (Volkov et al., 2012), Sentyabr'skoe (Nikolaev et al., 2013; Savva et al., 2016),

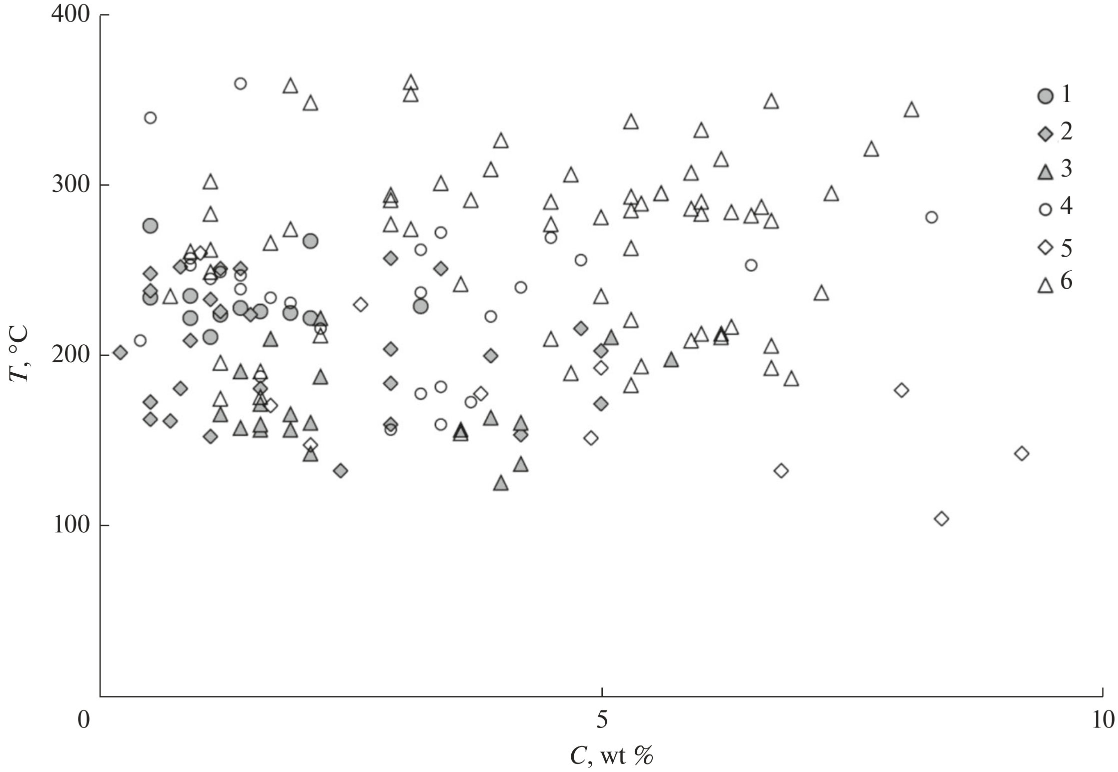

Fig. 6. The temperature–salinity diagram for mineral-forming fluids in the OChVB epithermal gold–silver deposits. (1) Kupol, (2) Dvoinoe, (3) Dzhul'etta, (4) Nyavlenga, (5) Tikhoe, (6) Sentyabr'skoe.

Nyavlenga (Volkov et al., 2014), Dzhul'etta (Prokof'ev et al., 2015), and Tikhoe deposits (Kolova et al., 2015).

The ore-forming fluids of most deposits had temperatures of 105–359°C and salinities of 0–9.2 wt %-equi NaCl. Higher temperatures (up to 435°C) and salinities (up to 37.0 wt %-equi NaCl) have only been recorded for fluids of the late mineralization phase on the Dukat deposit (Goncharov and Sidorov, 1979; Berman et al., 1993; Kravtsova, 2010). This phase is thought to have been related to the influence of a granitoid massif that was emplaced near the deposit. Some deposits were found to involve the action of heterogeneous fluids (Dukat and Sentyabr'skoe); this enables us to estimate the pressure that existed during the mineralization to be in the range 80–570 bars. These pressures are relevant to shallow and medium (subvolcanic) depths of mineralization.

Bulk analysis of the composition of fluid inclusions in quartz monofractions furnished data on fluid compositions for ten OChVB Au–Ag deposits (Table 5, Fig. 7): Dvoinoe, Kupol, Nyavlenga, Pepenveem, Pechal'noe, Dukat, Moroshka, Dal'nee, Dzhul'etta, and Tikhoe. The main components in the fluid include (g/kg H_2O): carbon dioxide (1.3–58.1), methane (0.02–3.18), chlorine (<0.1–5.15), sulfate ion (<0.3–21.65), hydrocarbonate ion (0–116.51), Na (0.79–23.90), K (0.16–18.79), Ca (0–4.70), and Mg (0–7.02). The following trace elements have been determined (mg/kg H_2O): Br (0–972.8), As (6.52–1921.4), Li (2.39–184.42), Be (0–0.19), B (38.85–7603.0), Rb (0–61.98), Cs (0–26.42), Sr (0–144.36), Mo (0–41.18), Ag (0–15.98), Sb (0.88–903.82), Cu (0–641.75), Zn (0–654.57), Cd (0–0.66), Pb (0–122.51), Bi (0–0.08), Th (0–0.20), U (0–0.10), Ga (0–0.59), Ge (0–1.01), Ti (0–12.74), Mn (0–1599.9), Fe (0–1772.2), Co (0–10.15), Ni (0–5.46), V (0–3.84), Cr (0–5.46), Y (0–4.50), Zr (0–1.20), Sn (0–3.09), Ba (0–33.65), W (0–184.64), Au (0–0.669), Hg (0–1.35), Tl (0–0.85) and REE (0.003–0.49). The ratios of the most typical components vary as follows: Na/K from 0.2 to 15.4, CO_2/CH_4 from 3.2 to 216.0, and K/Rb from 122.8 to 2725.5.

The analyses for the composition of mineral-forming fluids at the OChVB deposits are consistent with the results of cryometric studies: the fluids have low salinity and low concentrations of chlorine, carbon dioxide, and methane. The anions are dominated by the hydrocarbonate ion and, occasionally, by the sulfate ion, while the cations are dominated by sodium and potassium. Among the trace elements, one notes higher concentrations of Br, As, Li, B, Sb, Zn, and W.

The concentrations of cations and anions show a tendency of increasing K+ from earlier oreless quartz to productive quartz with increasing depth, as well as a slow decrease in the percentage of Na^+, Ca^{++}, and Cl. One observes a direct Ag–K correlation and an inverse

Table 5. The composition of solutions of the fluid inclusions in quartz sampled from ore veins from the OChVB Au–Ag deposits

Elements	Deposits													
	Dukat	Moroshka		Dal'nee		Dzhul'etta			Tikhoe					
	Duk-4	KW12-85	KW11-049	MSDL 43531004	MSDL 14481003	EV-1	EV-1	v-2c	Ti-1	304	290	Tikhii	Ti-1	Ti-7
Macrocomponents, g/kg water														
CO_2	2.91	3.80	5.74	2.98	4.27	11.23	6.15	6.89	11.84	31.10	24.24	9.24	25.99	19.46
CH_4	0.05	0.27	0.17	0.13	0.05	0.31	0.13	0.09	0.26	0.52	0.17	0.34	0.23	0.23
Cl^-	0.86	<0.5	0.58	2.14	6.13	2.69	0.57	2.52	3.37	2.53	5.15	0.54	3.60	4.17
SO_4^{2-}	<0.2	<1	<0.5	<0.5	<0.5	<0.3	0.31	<0.2	<0.3	<3	<1	<0.5	<0.5	9.22
HCO_3^-	6.84	18.30	6.57	6.77	10.50	4.11	1.35	0.53	0	84.19	28.42	13.29	12.19	10.20
Na	2.84	5.27	1.81	1.26	1.52	3.19	0.79	1.20	1.58	25.46	9.86	4.48	6.69	6.81
K	0.39	1.24	0.60	0.90	0.89	0.21	0.16	1.09	0.68	14.37	1.66	0.70	0.47	5.32
Ca	0.04	0.24	0.13	1.65	4.70	0	0.002	0	0	0	1.95	0.41	0	0.57
Mg	0.03	0.33	0.29	0.14	0.28	0	0	0.01	0.03	0	0.54	0	0	0.21
Microcomponents, 10^{-3} g/kg water														
Br	0	513.44	152.82	323.75	47.53	125.04	8.02	104.28	10.40	36.53	112.91	322.89	33.45	234.58
As	33.15	1072.7	66.55	111.98	183.62	28.32	16.18	26.80	105.15	1216.8	135.80	343.29	880.26	1807.3
Li	5.18	5.07	6.41	3.02	3.40	4.43	3.03	2.59	2.39	184.42	3.08	4.47	2.62	4.94
Be	0	0.09	0.10	0	0.05	0.06	0.05	0	0.08	0	0	0.19	0	0
B	143.59	4559.4	2223.0	853.55	896.08	67.18	240.28	68.72	38.85	9676.5	2233.2	4676.7	432.31	434.29
Rb	1.69	3.64	1.46	3.20	3.32	0.16	0	2.20	2.13	17.56	5.20	0	1.15	8.55
Cs	0.77	0.56	0.62	2.47	1.03	0.08	0	0.28	0.08	1.27	4.67	0	0.42	0.27
Sr	1.23	0.26	1.93	36.09	86.07	0	0	0	0.74	0	23.52	0	1.41	56.54
Mo	0.85	26.20	2.62	1.60	1.92	0	0.08	0	0.12	0	41.18	2.52	0.22	2.50
Ag	0	15.98	0	0	0.27	0.13	0	0.89	0.01	0	0	0	0.15	0
Sb	24.38	903.82	32.94	72.36	45.48	168.34	17.02	201.78	11.55	53.48	29.59	38.17	41.73	272.76
Cu	0	0.34	0.03	0	0	1.71	0	0	0.47	0	0	0.02	0	0.34
Zn	0	20.03	0	21.15	0	2.29	0	0	2.33	0	0	0	0	2.49
Cd	0	0.28	0	0	0.08	0.003	0	0.01	0	0	0.26	0.02	0	0.14

Table 5. (Contd.)

Elements	Deposits													
	Dukat	Moroshka		Dal'nee		Dzhul'etta			Tikhoe					
	Duk-4	KW12-85	KW11-049	MSDL 43531004	MSDL 14481003	EV-1	EV-1	v-2c	Ti-1	304	290	Tikhii	Ti-1	Ti-7
Pb	0.01	2.31	0	0	0	0	0.03	3.67	0.23	1.11	0	0	3.53	122.51
Bi	0	0	0	0	0	0.003	0	0	0.02	0	0	0	0	0
Th	0	0	0	0	0	0	0	0.05	0.03	0.20	0.09	0	0	0
U	0	0	0	0	0	0	0	0.01	0.01	0.10	0	0	0	0
Ga	0	0.12	0.70	0	0.59	0.10	0	0.19	0.22	0.23	0	0	0.20	0
Ge	0.05	0.10	0.19	0.13	0.06	0.09	0.18	0	0	0	0.19	0.37	0.17	0.83
Ti	0	0	0	3.50	12.74	0	0	4.29	0	0	0.60	0	0	5.95
Mn	8.64	1.64	0	29.48	86.02	0	0	0	1.55	0	118.63	0	0.54	10.66
Fe	4.30	82.39	0	0	30.10	0	0	8.98	32.55	0	0	0	0	19.36
Co	0	0	0	0.02	0.10	0	0	0	0.06	0	0.31	0	0.03	0.04
Ni	0	0	0.27	0.24	0.66	0.37	0.31	0	0	5.46	0	0.03	0.23	0.30
V	0	4.50	0.65	0	0	0.10	0.55	0.63	1.55	0.05	0.87	0	0	0
Cr	0.07	0.61	1.68	0.14	0.16	0.25	0	0.71	0.40	5.46	0	0	0.07	0
Y	0.01	4.50	0.65	0	0	0.01	0	0.06	0.02	0	0.87	0	0	0
Zr	0	0.04	0.29	0	0	0.03	0	1.20	1.07	0.04	0	0	0.05	0
Sn	0	0.10	0	0.03	0	0	0	0	1.36	3.09	0	0.04	0.02	0.003
Ba	0.13	3.43	0.34	1.40	19.12	0.07	0.17	1.17	1.95	33.65	0	0	0	5.89
W	9.08	11.03	9.35	4.44	1.78	0.01	0	0.25	2.94	33.65	11.48	4.02	0.24	2.44
Au	0	0.191	0.035	0	0	0.052	0.028	0.031	0.203	0.304	0.295	0.054	0	0.060
Hg	0	0.76	0.19	0.09	0.19	0	0	0.03	0	0	0	0	0	0.01
Tl	0	0.02	0.02	0.10	0.13	0.003	0	0.03	0	0.15	0	0	0.01	0.11
REE	0.03	0.05	0.12	0.07	0.04	0.003	0.03	0.17	0.05	0.06	0.24	0.14	0.01	0.07
Na/K	7.4	4.3	3.0	1.4	1.7	15.4	3.7	1.1	2.3	1.8	5.9	6.4	14.2	1.3
CO_2/CH_4	63.3	14.3	34.2	22.9	86.7	36.7	46.7	80.1	46.1	60.0	146.7	27.4	113.4	83.6
K/Rb	227.7	341.1	408.4	281.9	268.0	1281.9	–	494.7	317.5	818.6	319.6		409.4	621.8

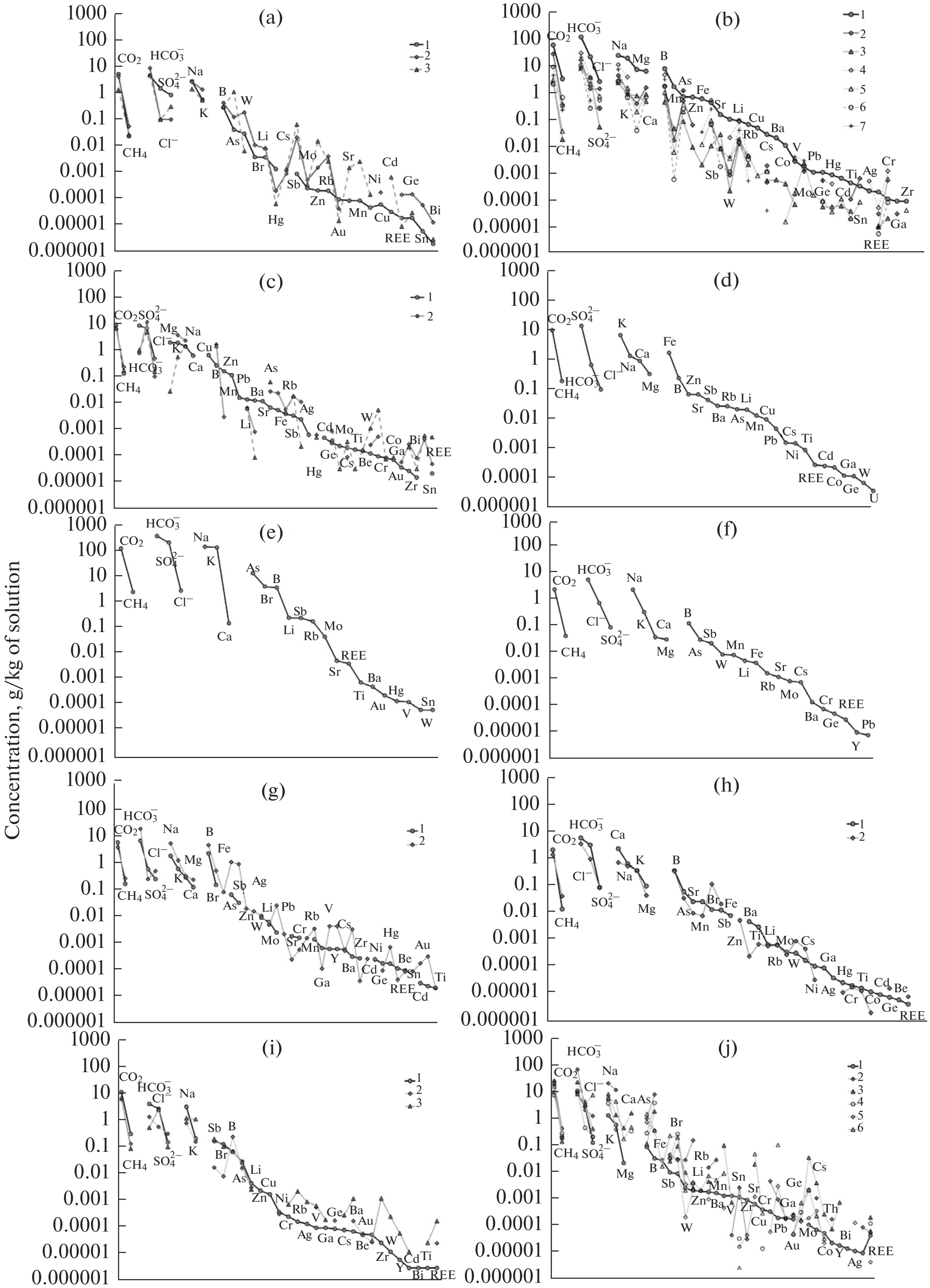

Fig. 7. The compositions of mineral-forming fluids in the OChVB gold–silver deposits. (a) Dvoinoe, (b) Kupol, (c) Nyavlenga, (d) Pepenveem, (e) Pechal'noe, (f) Dukat, (g) Moroshka, (h) Dal'nee, (i) Dzhul'etta, (j) Tikhoe.

Ag–Na correlation for productive quartz. The K/Rb ratio for solutions is generally high (occasionally reaching 2725), which may be evidence of an interaction between the ore-forming fluid and the host rocks. One occasionally encounters values below 250, which must most likely have resulted from a magmatic source of the fluid.

The most-pronounced feature that distinguishes the deposits studied here consists in sulfate concentrations in the fluid. One notes deposits with appreciable sulfate concentrations in the fluid (Dvoinoe, Kupol, Nyavlenga, Pepenveem, and Pechal'noe) and deposits with low sulfate concentrations (Dukat, Moroshka, Dal'nee, Dzhul'etta, and Tikhoe).

CONCLUSIONS

We conclude by noting that the ores of the OChVB epithermal Au–Ag deposits are characterized by an obvious enrichment in a wide range of elements compared with the mean upper crustal values.

Comparative analysis of the trace-element distributions in the ores studied here over classes of gold concentration shows a synchronous enrichment of the ores in similar sets of trace elements and allows indicator elements to be used to determine the type of ore-forming fluid.

The patterns identified here, viz., the prevalence of light lanthanoids over heavy ones and positive Eu anomalies, seem to be typical of the epithermal ore-forming system. The presence of Eu maxima in the REE distributions of epithermal ores is a characteristic feature of ore columns. The REE distributions of the ores studied here, as well as of the host rocks, are dominated by light "hydrophile" lanthanoids of the "cerium" set.

The epithermal ores studied here were mostly formed by fluids coming from depth (in the lower crust), as well as by solutions that were produced by deep fluids mixed with shallow infiltration waters. The fluid salinity increased toward later, low-temperature phases during the mineralization process. The ore-forming solutions are of the hydrocarbonate potassium type, having 60–80% hydrocarbonate and potassium of the total amount of cations and anions. The concentration of anions and cations shows a tendency of the potassium percentage to increase from the earlier oreless quartz toward productive quartz with increasing depth, as well as a slow decrease in the percentages of Na^+, Ca^{++}, and Cl^-. One observes a direct Ag–K correlation and an inverse Ag–Na correlation for productive quartz. The most-pronounced feature of the deposits studied here consists in sulfate concentrations in the fluid.

The results indicate magma chambers of andesite magmas and meteoric waters as the most likely sources of the fluids that went to form the epithermal Au–Ag ores in the OChVB deposits.

ACKNOWLEDGMENTS

This paper was written to fulfill the State Task at the IGEM RAN Metallogeny of Ore Areas in Volcano-Plutonic and Orogenic Fold Belts in Northeast Russia. The analyses were financially supported by the Russian Science Foundation, project no. 14–17–00170.

REFERENCES

Andreeva, E.D., *Genesis of Precious Metal Mineralization in the Central Kamchatka, Far East of Russia,* Doctoral Dissertation, Department of Natural History and Earth Science, Hokkaido University, 2013. 240 p. http://hdl.handle.net/2115/53927

Bau, M., Rare-earth element mobility during hydrothermal and metamorphic fluid-rock interaction and the significance of the oxidation state of europium, *Chem. Geol.,* 1991, vol. 93, pp. 219–230.

Belyi,V.F., *Geologiya Okhotsko-Chukotskogo poyasa* (The Geology of the Okhotsk–Chukchi Belt), Magadan: SVKNII DVO RAN, 1994.

Berman, Yu.S., Prokof'ev, V.Yu., Kozerenko, S.V., et al., The rejuvenation of gold–silver mineralization on the Dukat volcanogenic deposit: A study of fluid inclusions, *Geokhimiya,* 1993, no. 4: pp. 539–548.

Bortnikov, N.S., Gamyanin, G.N., Vikent'eva, O.V., et al., The composition and origin of fluids in the hydrothermal system of the Nezhdaninskoe gold deposit, Sakha-Yakutiya, Russia, *Geologiya Rudnykh Mestorozhdenii,* 2007, vol. 49, no. 2, pp. 99–145.

Egorov, V.N., Zhigalov, S.V., Volkov, A.V., et al., On rare-metal mineralization and comendites in the Khurchan–Orotukan metallogenic zone, *Dokl. Akad. Nauk*, 2005, vol. 405, no. 2, pp. 237–242.

Goncharov, V.I. and Sidorov, A.A., *Termobarogeokhimiya vulkanogennogo rudoobrazovaniya* (Thermal, Pressure, and Geochemical Conditions for Volcanogenic Mineralization), Moscow: Nauka, 1979.

Goryachev, N.A., Vikent'eva, O.V., Bortnikov, N.S., et al., The Natalkino worldclass gold deposit: REE distribution, fluid inclusions, stable oxygen isotopes, and the conditions during the formation of the ore (Northeast Russia), *Geol. Rudn. Mestor.,* 2008, vol. 50, no. 5, pp. 414–444.

Jones, B. and Manning, D.A.C., Comparison of geochemical indices used for the interpretation of palaeoredox conditions in ancient mudstones, *Chem. Geol.,* 1994, vol. 111, pp. 111–129.

Kolova, E.E., Volkov, A.V., Prokof'ev, V.Yu., et al., Properties of the ore-forming fluid that generated the Tikhoe epithermal Au–Ag deposit, Northeast Russia, *Dokl. Akad. Nauk,* 2015, vol. 463, no. 5, pp. 566–570.

Kolova, E.E., Volkov, A.A., Savva, N.E., et al., Mineralizxation on the Dvoinoe epithermal Au–Ag deposit, western Chukotka, *Dokl. Akad. Nauk,* 2018, vol. 478, no. 5, pp. 561–565.

Konstantinov, M.M., Natalenko, V.E., Kalinin, A.I., et al., *Zoloto-serebryanoe mestorozhdenie Dukat* (The Dukat Gold–Silver Deposit), Moscow: Nedra, 1998.

Kravtsova, R.G., *Geokhimiya i usloviya formirovaniya zolotoserebryanykh rudoobrazuyushchikh sistem Severnogo Priokhot'ya* (The Geochemistry and the Consitions of Generation for the Gold–Silver Mineralizing Systems in the Northern Coast of the Sea of Okhotsk), Novosibirsk: Akad. Izd-vo Geo, 2010.

Kravtsova, R.G. and Almaz, Ya.A., Rare earth elements in the ores of epithermal gold–silver and silver deposits, Northeast Russia, *Geokhimiya,* 2006, no. 12, pp. 1338–1344.

Kravtsova, R.G., Borovikov, A.A., Borisenko, A.S., et al., The conditions of generation for gold–silver deposits in the northern coast of the Sea of Okhotsk, Russia, *Geol. Rudn. Mestor.,* 2003, vol. 45, pp. 452–473.

Kravtsova, R.G., Zakharov, M.N., and Korkina, O.I., Rare earth elements in the metasomatites and ores of the Dukat gold–silver deposit, Northeast Russia, *Geol. Geofiz.,* 2005, vol. 46, no. 6, pp. 603–616.

Kryazhev, S.G., Prokof'ev, V.Yu., and Vasyuta, Yu.V., Using the ICP MS technique for the analysis of oreforming fluids, *Vestnik MGU, Seriya 4, Geologiya,* 2006, no. 4, pp. 30–36.

Kun, L., Ruidong, Y., Wenyong, Ch., et al., Trace element and REE geochemistry of the Zhewang gold deposit, southeastern Guizhou Province, China, *Chin. J. Geochem.,* 2014, vol. 33, pp. 109–118.

Lang, J.R., Baker, T., Hart, C.J., et al., An exploration model for intrusion related gold systems, *SEG Newsletter,* 2000, no. 40, pp. 6–15.

Mineev, D.A., *Lantanoidy v rudakh redkozemel'nykh elementov i kompleksnykh mestorozhdenii* (Lathanoids in Ores of Rare Earth and Complex Deposits), Moscow: Nauka, 1974.

Monecke, T., Kempe, U., and Gotze, J., Genetic significance of the trace element content in metamorphic and hydrothermal quartz: a reconnaissance study, *Earth. Planet. Sci. Lett.,* 2002, vol. 202, pp. 709–724.

Nikolaev, Yu.N., Prokof'ev, V.Yu., Apletalin, A.V., et al., Gold–telluride mineralization in western Chukotka: Mineralogy, geochemistry, and generation conditions, *Geol. Rudn. Mestor.,* 2013, vol. 55, no. 2, pp. 114–144.

Nolan, T.B., Epithermal precious-metal deposits of the western states, in *Lindgren volume*, New York: American Institute of Mining and Metallurgical Engineers, 1933, pp. 623–640.

Oreskes, N. and Einaudi, M.T., Origin of rare-earth element enriched hematite breccias at the Olympic Dam Cu-U-Au–Ag deposit, Roxby Downs, South Australia, *Econ. Geol.,* 1990, vol. 85, no. 1, pp. 1–28.

Prokof'ev, V.Yu., Volkov, A.V., Sidorov, A.A., et al., The geochemistry of the ore-forming fluid: The Kupol epithermal Au–Ag deposit, Northeast Russia, *Dokl. Akad. Nauk,* 2012, vol. 447, no. 4, pp. 433–436.

Prokof'ev, V.Yu., Ali, A.A., Volkov, A.V., et al., The geochemistry of the ore-forming fluid: The Dzhul'etta epithermal Au–Ag deposit, Northeast Russia, *Dokl. Akad. Nauk,* 2015, vol. 460, no. 3, pp. 329–333.

Sakhno, V.G., Barinov, N.N., Karas', O.A., et al., Petrologic and geochemical isotope criteria in the prediction of the extent of gold–silver potential for the volcanic struictures in the Chukotka sector of the Russian arctic coast, 2015. *http://www.ras.ru/FStorage/download.aspx?id=2104c42d-696d-4e2e-91e6-0e5d55f55ca2*

Savva, N.E., Volkov, A.V., and Sidorov, A.A., Thermal metamorphism in the epithermal Au–Ag ores of the Nyavlenga deposit, Northeast Russia, *Dokl. Akad. Nauk,* 2007, vol. 413, no. 5, pp. 655–660.

Savva, N.E., Kolova, E.E., Fomina, M.I., et al., Gold polymetal mineralization in explosive breccias: mineralogic and genetic aspects (the Sentyabrskoe deposit, Northeast, Chukotka), *Vestnik SVNTs DVO RAN,* 2016, no. 1, pp. 16–36.

Sidorov, A.A., Belyi, V.F., Volkov, A.V., et al., The conditions for the generation of a unique gold–silver deposit, western Chukchi Peninsula, *Dokl. Akad. Nauk,* 2007, vol. 414, no. 2, pp. 234–239.

Sidorov, A.A., Belyi, V.F., Volkov, A.V., et al., The Gold–Silver Okhotsk–Chukchi Volcanogenic Belt, *Geologiya Rudnykh Mestorozhdenii,* 2009, vol. 51, no. 6, pp. 512–527.

Sidorov, A.A., Volkov, A.V., Chekhov, A.D., Savva, N.E., Alekseev, V.Yu., and Uyutnov, K.V., Volcanogenic belts of the marginal sea lithosphere in the Russian Northeast and their ore potential, *J. Volcanol. Seismol.,* 2011, vol. 5, no. 6, pp. 386–398.

Sidorov, A.A., Volkov, A.V., and Alekseev, V.Yu., Zones of activation and volcanism, *J. Volcanol. Seismol.,* 2013, vol. 7, no. 3, pp. 185–195.

Takahashi, R., Matsueda, H., Okrugin, V.M., et al., Epithermal gold-silver mineralization of the Asachinskoe deposit in South Kamchatka, Russia, *Resource Geology,* 2007, vol. 57, no. 4, pp. 354–373.

Taylor, S.R. and McLennan, S.M., *The Continental Crust: Its Composition and Evolution,* Blackwell Scientif. Publs., Oxford, 1985.

Tikhomirov, P.L., Kalinina, E.A., Kobayashi, K., et al., Late Mesozoic silicic magmatism of the North Chukotka area (NE Russia): Age, magma sources, and geodynamic implications, *Lithos,* 2008, vol. 105, pp. 329–346.

Tikhomirov, P.L., Kalinina, E.A., Moriguti, T., et al., Trace element and isotopic geochemistry of Cretaceous magmatism in NE Asia: Spatial zonation, temporal evolution, and tectonic controls, *Lithos,* 2016, vol. 264, pp. 453–471.

Vinokurov, S.F., Europium anomalies in ore deposits and their genetic significance, *Dokl. Akad. Nauk,* 1996, vol. 346, no. 6, pp. 792–795.

Vinokurov, S.F., Kovalenker, V.A., Safonov, Yu.G., et al., Lanthanoids in the quartz of epithermal gold deposits: The distribution and genetic significance, *Geokhimiya,* 1999, no. 2, pp. 171–180.

Volkov, A.V. and Sidorov, A.A., Deposits in the volcanogenic belts of Northeast Asia: A raw base for the development of new ore mining areas, *Vestnik RAN,* 2012, no. 1, pp. 29–35.

Volkov, A.V., Savva, N.E., Sidorov, A.A., et al., Patterns in the location of and the environments in the generation of Cu-Au porphyry deposits in the Russian northeast, *Geol. Rudn. Mestorozhd.,* 2006, vol. 48, no. 6, pp. 512–539.

Volkov, A.V., Prokof'ev, V.Yu., Savva, N.E., et al., Mineralization on the Kupol gold–silver deposit, Northeast Russia: A study of fluid inclusions, *Geol. Rudn. Mestor.,* 2012, vol. 54, no. 4, pp. 350–359.

Volkov, A.V., Sidorov, A.A., and Starostin, V.I., *Metallogeniya vulkanogennykh poyasov i zon aktivizatsii* (Metallogeny in Volcanogenic Belts and Activation Zones), Moscow: OOO MAKS Press, 2014.

Volkov, A.V., Savva, N.E., Sidorov, A.A., et al., The Agan epithermal gold–silver deposit and perspectives for detecting mineralization of the high-sulfidation type in Northeast Russia, *Geologiya Rudnykh Mestorozhdenii,* 2015, vol. 57, no. 1, pp. 25–47.

Volkov, A.V., Sidorov, A.A., Savva, N.E., et al., Epithermal mineralization in the Kedon paleozoic volcano-plutonic belt, Northeast Russia: Geochemical studies of Au–Ag mineralization, *J. Volcanol. Seismol.,* 2017a, vol. 11, no. 1, pp. 1–19.

Volkov, A.V., Sidorov, A.A., Savva, N.E., Kolova, E.E., Chizhova, I.A., and Murashov, K.Yu., The geochemistry of volcanogenic mineralization in the northwestern segment of the Pacific Ore Belt: Northeast Russia, *J. Volcanol. Seismol.,* 2017b, vol. 11, no. 6, pp. 389–406.

Zharikov, V.A., Gorbachev, N.S., Latfutt, P., et al., The distribution of rare earth elements and yttrium between the fluid and the basaltic melt at pressures of 1–12 kbars (experimental evidence), *Dokl. Akad. Nauk,* 1999, vol. 366, no. 2, pp. 239–241.

Translated by A. Petrosyan